Corrosion Science xxx (xxxx) xxx–xxx

Contents lists available at ScienceDirect

Corrosion Science

journal homepage: www.elsevier.com/locate/corsci

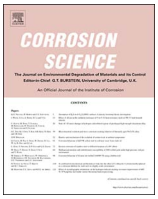

Benzotriazole and cerium chloride as corrosion inhibitors for AA2024-T3: An EIS investigation supported by SVET and ToF-SIMS analysis

L.B. Coelho[a], D. Cossement[b], M.-G. Olivier[a,b,*]

[a] *Materials Science Department, Faculty of Engineering, University of Mons, 20 Place du Parc, 7000 Mons, Belgium*
[b] *Materia Nova asbl, Avenue Copernic 1, 7000 Mons, Belgium*

ARTICLE INFO

Keywords:
A. Aluminium
A. Rare earth elements
B. EIS
B. SIMS
C. Neutral inhibition

ABSTRACT

The inhibitive effects provided by benzotriazole (BTA) and cerium chloride ($CeCl_3$) on 2024-T3 aluminium alloy were assessed, individually and combined, in 0.05 M NaCl electrolytes, by means of Electrochemical Impedance Spectroscopy (EIS). From the analysis of impedance fitted parameters, a synergistic effect appears to exist between both inhibitors until 14 days of immersion. The Scanning Vibrating Electrode Technique (SVET) was applied to an Al/Cu galvanic coupling model in order to better comprehend the observed inhibitive actions. Additionally, Time of Flight Secondary Ion Mass Spectrometry (ToF-SIMS) was employed to evaluate the in-depth distribution of species related to the inhibitive film/alloy interface.

1. Introduction

The localised corrosion of 2xxx aluminium alloys in NaCl media endures as a major issue in aeronautics. Probably the most well-known member of the 2000 series, the AA2024 is a class of precipitation hardened aluminium alloys with a high strength-to-weight ratio [1]. It is well known that most of the AA2024 precipitates, such as Al-Cu and Al-Cu-(Fe,Mn) containing intermetallics, act as cathodes in an anodic Al matrix [2–6]. Therefore, according to the results of several authors [1,2,7–10], the driving force for localised corrosion processes is the micro-galvanic couplings formed between the matrix and the Cu-rich IMPs. In near-neutral aerated solutions, the Cu-rich cathodic sites enhance the oxygen reduction reaction (ORR).

The localised dissolution of the Al matrix often results in crevice formation around almost unattacked particles, constituting the so-called trenching mechanism [2,6,7,11]. Next, the Cu-rich particles are able to pass into solution, becoming subjected to free corrosion conditions [2,10]. Copper is then reduced and redeposited on the top of other IMPs, leading to copper "refining" processes [12]. Concerning the Al_2CuMg phase, it is considered to be less noble than the matrix and is thus subjected to anodic attack [2,9,10]. Lacroix et al. [13,14], using SKPFM, were able to show that Al and Mg are selectively dissolved from the S-phase, leaving behind a Cu sponge-like material. In a next step, this Cu-enriched phase constitutes cathodes that are also likely to be subject to the trenching process [2,5,9,10].

The aeronautical industry has an urgent interest in corrosion inhibitors because of the environmental regulations concerning hexavalent chromium. Although an official sunset date for the use of Cr(VI) has not yet been settled, the European Chemicals Agency has allowed a number of industries in aerospace sector to use it for longer than 2019 under strict conditions [15,16]. Therefore, attempts have been made to achieve hexavalent chrome-free approaches for the protection of AA2024 [1,9,17,18]. Benzotriazole (BTA) [1,9,17,19] and cerium salts [4,20] have shown very promising results for inhibiting corrosion on AA2024 in neutral NaCl solutions. Zheludkevich's EIS study [1] suggested that a thin BTA-based layer is formed on the alloy surface, protecting it from corrosion after the first hours of exposure.

Rare-earth elements have also proven to be one the most promising inhibitors of Al corrosion, thanks to the pioneering works of Hinton et al. [21,22]. It is generally accepted that Ce ions lead to the precipitation of insoluble cerium oxides/hydroxides that hinder corrosion reactions. The presence of Ce^{3+} and OH− in an aqueous solution allow the precipitation of a protective $Ce(OH)_3$ phase (Eq. (1)) [21,23]. Regarding AA2024, the local pH increase around IMPs triggers the precipitation reaction between Ce^{3+} species and the hydroxyl ions [4]. Once the cathodic particles are blocked, the cerium deposition can be extended towards regions that were initially anodic [24,25].

As corrosion and inhibition processes usually comprise local cells formed on an active surface, an ideal comprehension of their mechanisms would demand in situ analyses at the lowest possible scales [9,26]. In particular, the Scanning Vibrating Electrode Technique (SVET) has emerged as a monitoring tool convenient for galvanic corrosion inhibition analyses [9,24,26–28]. In a previous SVET investigation [29], an Al/Cu galvanic coupling model was employed to simulate the micro-galvanic coupling typical of AA2024. By using this model, a positive synergistic effect between benzotriazole and cerium chloride was

---

[*] Corresponding author at: Materials Science Department, Faculty of Engineering, University of Mons, 20 Place du Parc, 7000 Mons, Belgium.

https://doi.org/10.1016/j.corsci.2017.11.004
Received 19 June 2017; Received in revised form 16 October 2017; Accepted 3 November 2017

Please cite this article as: Coelho, L.B., Corrosion Science (2017), http://dx.doi.org/10.1016/j.corsci.2017.11.004

revealed. It is fundamental to mention that neither BTA nor $CeCl_3$ are restricted under REACH regulation [30,31].

Multifunctional inhibitor systems composed of inorganic cations (rare earths) acting as cathodic inhibitors, and organic anions acting as anodic inhibitors, have recently shown encouraging results [32–35]. The synergistic effect of mixing different inhibitors, in the matter of corrosion protection of galvanically coupled metals, has been increasingly researched. Marcelin's EIS investigation demonstrated the synergistic effect of 8-hydroxyquinoline and BTA on an Al/Cu galvanic couple model and on AA2024 [36]. Kallip's local investigation highlighted fine results for Zn/Fe galvanic coupling by mixing BTA and cerium nitrate [27]. Snihirova et al. [37] observed synergistic effects by mixing salicylaldoxime and Ce(III) for the protection of an Al-Cu-Mg sample simulating the S-phase in AA2024.

The aim of the present study is to evaluate the efficiency of an inhibitor system, so far only tested on an Al/Cu galvanic pair model with promising results [29], on actual AA2024-T3 samples. For this purpose, Electrochemical Impedance Spectroscopy was employed in a 0.05 M NaCl reference solution containing BTA and/or $CeCl_3$ for 14 days. Furthermore, the same Al/Cu model previously considered was analysed by SVET in order to better comprehend some of the outcomes found for the alloy. ToF-SIMS was used to reveal the depth profiling of the protective film species, while SEM-EDX analysis was applied to investigate the corroded surfaces. Finally, this work aspires to invoke the importance of considering simplified model systems (together with the actual materials) for studying the corrosion protection approaches for complex alloys.

2. Materials and methods

2.1. Electrochemical impedance spectroscopy (EIS)

Electrochemical impedance spectroscopy (EIS) measurements were applied to assess the inhibitive effects of BTA and cerium chloride, separately and combined, on AA2024-T3 samples (Q-Lab). The main elements of the purchased Al alloy were Cu (3.8–4.9 wt.%), Mg (1.2–1.8 wt.%) and Mn (0.3–0.9 wt.%). EIS measurements were performed with a computer controlled AMETEK Parstat 2273 (Powersuite® software) connected to an electrochemical interface. A conventional three-electrode configuration was employed under aerated conditions. The counter electrode was a platinum wire and all potentials were measured with respect to an Ag/AgCl/KClsat (+197 mV/ENH) reference electrode. The exposed surface of the working electrode was 7.07 cm^2. Samples were placed in a Faraday cage to avoid electromagnetic interferences. A 5 mV RMS amplitude signal voltage (vs OCP) was applied at different frequencies, ranging from 100 kHz to 10 mHz, with 10 frequencies per decade. AA2024-T3 substrates were analysed in a 0.05 M NaCl reference solution with different concentrations of benzotriazole (≥98.0%, Merck) and $CeCl_3\,7H_2O$ (≥98.5%, Fluka Chemika). When working with $CeCl_3$, the NaCl concentration was altered to keep the final Cl^- concentration at 0.05 M. The substrates were degreased prior to use in an alkaline aqueous solution containing 52.5 g/L of TURCO TM 4215 for 12 min at 50 °C. The OCP was followed for 45 min prior to EIS measurements in order to ensure that stationary conditions were reached. Samples remained immersed for up to two weeks and each measurement was repeated at least twice.

2.1.1. Equivalent electrical circuit fitting from impedance data

In the absence of inhibitors, an Electrical Equivalent Circuit (EEC) composed of an $R_{ox}//CPE_{ox}$ element was proposed to describe the behaviour of bare AA2024 in NaCl electrolyte (Fig. 1(a)) [36]. As long as the passive layer does not continuously cover the surface (due to the presence of IMPs) its capacitive behaviour (CPE_{ox}) was considered in parallel with a resistive response (R_{ox}). A Constant Phase Element (CPE) was considered instead of pure capacitance (C is a frequency dependent term and can be described by Eq. (2) [1]). In inhibitors-containing solutions, in order to take into account the presence of the time constant (TC) related to the inhibitive film, an additional $R_f//CPE_f$ circuit was introduced (Fig. 1(b)). The R_f is the resistance of the inhibitor film while CPE_f is the constant phase element related to its capacitance [38]. The two parts of the circuit were imbricated to follow the hypothesis that the presence of an inhibitor would decrease the active surface in contact with the electrolyte. Such a model has been used in different investigations to account for the impedance contribution of cerium [39,40] and BTA [1,36] on AA2024. Since all considered impedance spectra presented quite noisy data between 10^{-1} and 10^{-2} Hz, the low frequency TC related to the polarisation resistance/double layer capacitance was not considered in the fitting procedure. The experimental EIS data were fitted according to the ECC models by using Zview software. The n parameter values associated with CPE_{ox} and with CPE_f were between 0.77 and 1.00. Finally, based on the MPEC procedure presented in [33], the relative errors for each frequency point were calculated and variations never exceeded 5% for Z' and |Z| parameters.

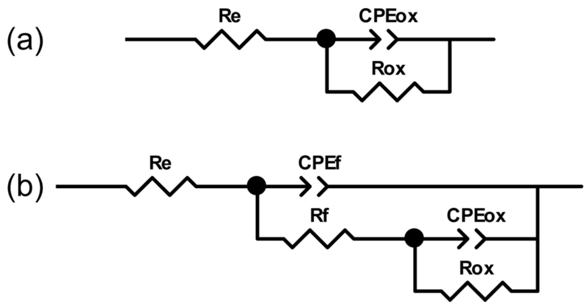

Fig. 1. Equivalent Electrical Circuits used to fit the impedance data for AA2024 in: (a) 0.05 M NaCl solution and (b) 0.05 M NaCl reference solution with BTA and/or $CeCl_3$. R_e: electrolyte resistance; R_f: resistance of the inhibitive film; CPE_f: parameter associated with the capacitive properties of the inhibitive film; R_{ox}: Resistance associated with the oxide film; CPE_{ox}: parameter associated with the capacitive properties of the oxide film.

2.2. Scanning vibrating electrode technique

SVET was applied with the aim of better understanding the inhibitive mechanisms of benzotriazole and cerium chloride on AA2024. For this purpose, an Al/Cu galvanic coupling model was constructed to simulate the galvanic corrosion characteristic of AA2024 [29]. Cu and Al rods (2 mm in diameter, 99.99% purity, Goodfellow) were mounted with a 2 mm gap between them. The electrical connection was made at the rear of the mounting by Sn welding. Prior to the SVET measurements, the sample surface was ground using SiC paper (up to the 2000 grades) and was consecutively rinsed with ethanol, distilled water and dried with compressed air. The equipment employed was a commercial Perkin Elmer SVP100 (Uniscan). Every test was repeated at least twice. The SVET probe (Pt, Ø = 50 μm) was placed 150 μm from the sample surface and measurements were taken with a vibration amplitude equal to 50 μm (peak-to-peak). The scan area was 10 mm x 7.5 mm, the step size was 78.8 μm and the scan speed was 1000 μm/s.

A near-neutral aerated 12.00 mM NaCl electrolyte (pH ≈ 6, conductivity $k \approx 1300\ \mu S\ cm^{-1}$) was chosen as a reference solution [17,24,41]. The pH and conductivity of the 12.00 mM NaCl solution did not change in the presence of 1.75 mM BTA. The chloride salt was selected in order to isolate the effect of cerium [4,23,24]. Nevertheless, the addition of $CeCl_3\,7H_2O$ imports extra chloride ions into the solution (the same for $CuCl_2.2H_2O$). In these cases, the NaCl concentration was modified in order to keep the total chloride concentration equal to 12.00 mM, the same level as the reference electrolyte. By doing so, the pH and conductivity of the solutions remained unaltered in the presence of the studied cerium chloride (1.25 and 4.00 mM) and copper chloride (1.75 mM) concentrations.

Distinct procedures can be envisaged to attain quantitative information from SVET data; namely, the maximum height of the anodic/